Assumption-Independent Single-Particle Wave Functions for Positrons in Solids: Applications to Angular Distributions in Al and Si†

D. STROUD AND H. EHRENREICH
Division of Engineering and Applied Physics, Harvard University, Cambridge, Massachusetts

(Received 12 February 1968)

The single-particle positron wave function in a solid may be calculated by a new technique which is entirely free of any theoretical assumptions by virtue of its use of experimental x-ray form factors to construct the potential. The results obtained accordingly form an excellent starting point for a systematic treatment of many-body effects in electron-positron annihilation processes. The positron wave function, which has the full crystal symmetry, is used together with pseudopotential wave functions for the valence electrons to compute the angular distribution of annihilation radiation from Al and Si for several crystal orientations. Agreement with experiment is excellent. The angular distribution from Al is found to be practically isotropic, despite the angular variation of the positron wave function. The substantial anisotropy in Si is reproduced within experimental error. Use of a constant positron wave function somewhat reduces the agreement. The calculated curves are little affected, however, by appreciable changes in the pseudopotential coefficients, indicating that positron annihilation is an insensitive probe of semiconductor band structures. The validity of using pseudopotential electron wave functions in the present context is discussed. The approximation is found to be excellent for most of the angular distribution because the positron is largely excluded from the core, where pseudo-wave-functions are incorrect. Accordingly, unlike positron lifetimes, the angular distribution can be well explained by an independent-particle model, even when it displays considerable anisotropy.

I. INTRODUCTION

THE annihilation of positrons in solids has been found to be a useful probe for obtaining information about the momentum distribution of the electrons.[1] However, in contrast to photon probes, for example, positrons perturb the system appreciably and are able to sample effectively only the valence electrons.[2,3] Because of their positive charge, electrons tend to pile up around the positron, thus disturbing their normal spatial distribution in the solid. Such many-electron effects are treated accurately only with great difficulty.[4–7] However, while they can shorten the positron lifetime appreciably, the electron-positron correlations fortunately appear to influence the angular distribution of the γ rays much less appreciably,[4,5,8] and for that reason the experimental results are useful in providing information about the solid.

Positrons are repelled by the positively charged atomic cores, their wave functions therefore being concentrated in the outer parts of the unit cell. This effect, which would be present even if the positrons were test charges without the consequent many-electron effects, causes the positrons to annihilate predominantly with the valence electrons. The resultant spatial variation of the positron wave function can also influence the annihilation significantly and should be known accurately within the limits of band theory if the extracted information concerning the electrons is to be reliable.

This latter aspect of the problem has not yet been treated completely adequately.[3,8,9] The present paper suggests an approach that permits the calculation of the positron wave function in the single-particle approximation in a manner which is *completely free of any theoretical assumptions*. That such assumptions can, in fact, be avoided follows from the close relationship of the x-ray form factors to the Fourier coefficients of the potential seen by the positron. It is, of course, just such Fourier components with respect to reciprocal lattice vectors that enter directly into the secular equation that determines the energies and wave functions. More specifically, the positron potential results from a part due to the nuclei and another part resulting from the electrons, both components being purely Coulombic in nature. The nuclear part may be expressed in terms of point charges situated at the lattice sites. Its Fourier coefficients are easily found. The corresponding coefficients of the electron part, however, can be expressed directly in terms of the x-ray form factor with the help of Poisson's equation. This avoids the necessity of ever calculating directly the electronic spatial distribution in the construction of the secular equation. This element of simplicity stands in sharp contrast to the situation encountered in the calculation of electron band structures, where there exist no experimental probes that determine the corresponding electronic part.

The solution of the resulting secular equation is especially simple because the positron can be assumed

† Supported in part by the National Science Foundation under Grant No. GP-5321 and the Advanced Research Projects Agency.

[1] Extensive lists of references and many review articles may be found in *Proceedings of the Conference on Positron Annihilation*, edited by A. T. Stewart and L. O. Roellig (Academic Press Inc., New York, 1966).

[2] S. DeBenedetti, C. E. Cowan, W. R. Konneker, and H. Primakoff, Phys. Rev. **77**, 205 (1950).

[3] R. A. Ferrell, Rev. Mod. Phys. **28**, 308 (1955).

[4] S. Kahana, Phys. Rev. **129**, 1622 (1963).

[5] J. P. Carbotte and S. Kahana, Phys. Rev. **139**, A213 (1965).

[6] J. P. Carbotte, Phys. Rev. **144**, 309 (1966).

[7] J. Crowell, V. E. Anderson, and R. H. Ritchie, Phys. Rev. **150**, 243 (1966); other references cited in Refs. 4–7.

[8] S. Berko and J. S. Plaskett, Phys. Rev. **112**, 1877 (1958).

[9] E. Daniel, J. Phys. Radium **18**, 691 (1957).

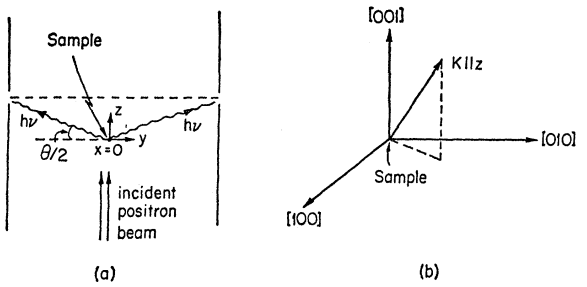

FIG. 1. (a) Schematic of parallel-slit apparatus. (b) Diagram showing the relationship of $\mathbf{K}$ to the principal axes of a cubic crystal.

to thermalize in a time short compared to its lifetime.[10] As a consequence, only the Γ_1 ($\mathbf{k}=0$) state of the positron band structure need be considered.

The computation of the annihilation rate requires knowledge of the electronic wave function as well. This paper suggests that for solids with small cores, like Al and Si, it suffices to use pseudopotential[11–14] wave functions for this purpose. Such wave functions differ from their correct counterparts only in the core region from which the positron is essentially excluded.

Detailed application of these ideas in calculations of the annihilation rate of positrons in Si and Al exhibit remarkably good agreement with experiment.[8,15,16] In particular, the fact that the calculations are able to reproduce excellently the Si experimental angular distribution, which depends significantly on the crystallographic orientation of the crystal, indicates that the present independent-particle approach coupled with the use of electron pseudo-wave-functions has merit, at least for the simpler solids. More importantly, because of its relatively few assumptions, the present theory is likely to yield a reliable single-particle description of positron annihilation. As a consequence, it represents an excellent starting point for a systematic many-particle description of the process, since significant deviations from the experimental angular distributions can be ascribed to positron-electron and electron-electron interactions.

The details of the formalism are described in Sec. II of the present paper. The results for Al and Si are discussed in Secs. III and IV, respectively.

[10] G. E. Lee-Whiting, Phys. Rev. **97**, 1557 (1955).
[11] D. Brust, Phys. Rev. **134**, A1337 (1964).
[12] M. L. Cohen and T. K. Bergstresser, Phys. Rev. **141**, 789 (1966).
[13] E. O. Kane, Phys. Rev. **146**, 558 (1966).
[14] W. A. Harrison, *Pseudopotentials in the Theory of Metals* (W. A. Benjamin, Inc., New York, 1966).
[15] J. C. Erskine and J. D. McGervey, Phys. Rev. **151**, 615 (1966).
[16] J. C. Erskine (private communication). We are grateful to Dr. Erskine for making these unpublished data available, which are in substantial agreement with those previously published in Ref. 15.

II. FORMALISM

In the independent-particle approximation, the probability that an annihilation event will yield two photons of total momentum p is proportional to[17]

$$f(\mathbf{p})=\sum_{kl} n_{kl}\left|\int d^3r\,\exp(-i\mathbf{p}\cdot\mathbf{r}/\hbar)\psi_+(\mathbf{r})\psi_{kl}(\mathbf{r})\right|^2, \quad (1)$$

where ψ_+ is the positron ground-state wave function, ψ_{kl} is the electron wave function corresponding to wave number $\mathbf{k}$ and band index l, and n_{kl} is the occupation number for the state $\mathbf{k}$, l. ($n_{kl}=1$ if $\mathbf{k}l$ is occupied and 0 if it is not.) The counting rate measured by the standard parallel-slit apparatus is proportional to

$$F_K(\theta)=\int_{-\infty}^{\infty}\int_{-\infty}^{\infty} dp_x dp_y f(p_x, p_y, p_z) \quad (2)$$

for $p_z=mc\theta/\hbar$. The angle θ and reciprocal lattice vector $\mathbf{K}$ are defined in Fig. 1.

In order to predict the counting rate it is necessary to have a means for calculating electron and positron wave functions. In this section the formalism necessary for computing ψ_+ from the x-ray form factors will be developed. In addition, explicit forms for $f(\mathbf{p})$ in terms of these and pseudo-wave-functions approximating the ψ_{kl} will be exhibited. Expressions suitable for estimating the magnitude of the core contribution will also be noted. For simplicity the treatment will be restricted to solids having one atom per unit cell although many of its features apply to more complicated solids. The extension of this treatment to the diamond structure

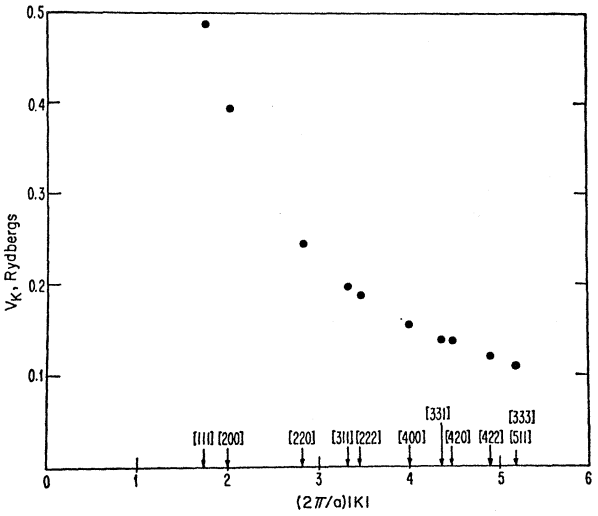

FIG. 2. Fourier coefficients V_K of the positron potential in Al, versus $(2\pi/a)\,|\mathbf{K}|$. (a=fcc cube edge, $\mathbf{K}$=reciprocal lattice vector.)

[17] P. R. Wallace, in *Solid State Physics*, edited by F. Seitz and D. Turnbull (Academic Press Inc., New York, 1960), Vol. 10, pp. 1–46.

will be given in connection with the discussion concerning Si in Sec. IV.

The positron moves in the Coulomb field of the nuclei and electrons. The corresponding potential may be written, in atomic units, as

$$V(\mathbf{r})=2\int\frac{d^3r'\,\rho(\mathbf{r}')}{|\,\mathbf{r}-\mathbf{r}'\,|},\tag{3}$$

where

$$\rho(\mathbf{r})=\rho^+(\mathbf{r})+\rho^-(\mathbf{r})\tag{4}$$

is the total charge density at $\mathbf{r}$, $\rho^+(\mathbf{r})$, and $\rho^-(\mathbf{r})$ representing the nuclear and electronic components, respectively. Evidently ρ^- is always negative. Since $V(\mathbf{r})$ and $\rho(\mathbf{r})$ are periodic, their Fourier components

$$V_{\mathbf{K}}=v_a^{-1}\int_{v_a}d^3r\;V(\mathbf{r})\;\exp(i\mathbf{K}\cdot\mathbf{r}),$$

$$\rho_{\mathbf{K}}=v_a^{-1}\int_{v_a}d^3r\;\rho(\mathbf{r})\;\exp(i\mathbf{K}\cdot\mathbf{r})$$

are nonvanishing only at reciprocal lattice vectors $\mathbf{K}$ and the integrals need be carried only over the unit-cell volume v_a. The transformed expressions corresponding to Eqs. (3) and (4) are

$$V_{\mathbf{K}}=8\pi\rho_{\mathbf{K}}/\mathbf{K}^2,\tag{5}$$

$$\rho_{\mathbf{K}}=\rho_{\mathbf{K}}{}^+{+}\rho_{\mathbf{K}}{}^-.\tag{6}$$

Equation (5) expresses the Fourier components of the potential very simply in terms of those for the charge density. Since the nuclear charge Z can be expressed as a δ function at the origin of each cell,

$$\rho_{\mathbf{K}}{}^+=Z/v_a.\tag{7}$$

The transformed electron charge density is more difficult to calculate from first principles, but, as already emphasized, it is easily determined from experimental information. The intensity of an x-ray diffraction line is expressible as a product of the incident intensity, a geometrical factor, the Debye-Waller factor, and $|\,\rho_{\mathbf{K}}{}^-\,|^2$.[18] Accordingly, $|\,\rho_{\mathbf{K}}{}^-\,|$ will be determined by the measurement of an appropriate line. The determination of the phases of the $\rho_{\mathbf{K}}{}^-$ represents a separate problem, which, however, is well understood and easily solved for the vast majority of crystal structures.[19] In crystals with inversion symmetry, the $\rho_{\mathbf{K}}{}^-$ must be real and the problem reduces to one of determining sign. The present considerations will be restricted to this case, since even Si possesses inversion symmetry. Unambiguous methods for sign determination are available.

[18] See, for example, W. H. Zachariasen, *Theory of X-Ray Diffraction in Crystals* (John Wiley & Sons, Inc., New York, 1945).

[19] A general discussion is given by J. Bouman, *International Tables for X-Ray Crystallography* (Kynoch Press, Birmingham, 1959), Vol. 2, pp. 358–359. The applications to Al and Si are presented in detail in the Ph.D. dissertation of D. Stroud, Harvard University (unpublished).

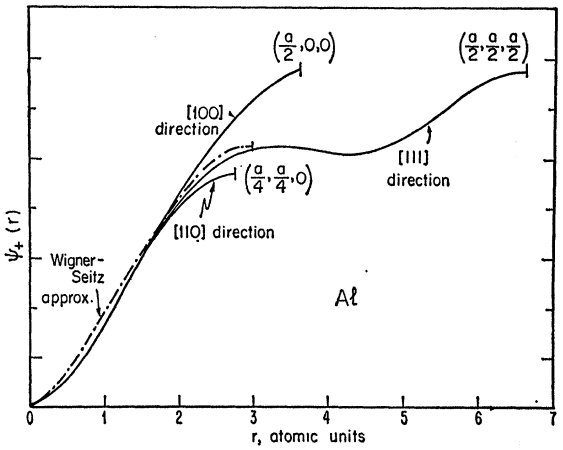

FIG. 3. Positron wave function in Al in arbitrary units. The solid lines represent the wave function obtained in the present calculation, and are extended as far out as the appropriate boundary of the Wigner-Seitz cell. The dashed line corresponds to the spherically symmetric wave function in the Wigner-Seitz approximation of Ref. 8, and is plotted to the boundary of the Wigner-Seitz sphere.

They are easily applied to Al.[19] However, plausibility arguments often suffice. For example, a graph of the experimentally determined $|\,\rho_{\mathbf{K}}{}^-\,|$ versus $\mathbf{K}$ generally shows that a smooth curve can be drawn through the data points only if the $\rho_{\mathbf{K}}{}^-$ all have the same sign. Since $\rho_0{}^-=-Z/v_a$ is just the average electron charge density, that sign must be negative. On the other hand, the Fourier components of the total charge density $\rho_{\mathbf{K}}$ as given by Eq. (6) are all positive in crystals having inversion symmetry, because in this case one may write

$$\rho_{\mathbf{K}}=v_a^{-1}\left(Z-\int_{v_a}d^3r\,|\,\rho^-(\mathbf{r})\,|\,\cos\mathbf{K}\cdot\mathbf{r}\right)$$

$$\geq v_a^{-1}\left(Z-\int_{v_a}d^3r\,|\,\rho^-(\mathbf{r})\,|\right)\geq 0.$$

When $\mathbf{K}=0$, the expression (5) for $V_{\mathbf{K}}$ becomes undefined. This is of no practical importance because V_0 merely adds a constant to the energy eigenvalue and does not affect the positron wave function.

The Fourier components $V_{\mathbf{K}}$ appropriate for Al, shown in Fig. 2, are consistent with the preceding conclusions. These components determine the positron wave function. Substitution of a plane-wave expansion for the $\mathbf{k}=0$ state,

$$\psi_+(\mathbf{r})=\Omega^{-1/2}\sum_{\mathbf{K}}a_{\mathbf{K}}\exp(i\mathbf{K}\cdot\mathbf{r}),\tag{8}$$

into the Schrödinger equation yields

$$\sum_{\mathbf{K}'}[(\mathbf{K}^2-E)\delta_{\mathbf{K},\mathbf{K}'}+V_{\mathbf{K}-\mathbf{K}'}]a_{\mathbf{K}'}=0.\tag{9}$$

Here Ω represents the volume of the crystal, and the expansion coefficients $a_{\mathbf{K}}$ are normalized so that

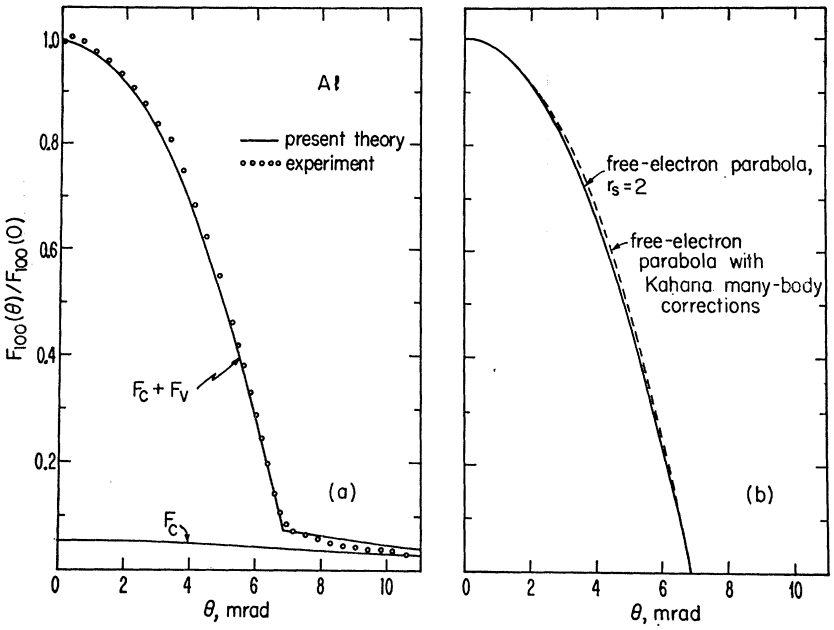

FIG. 4. (a) Normalized computed and measured angular distribution of annihilation γ-ray pairs in Al. The experimental points are data by S. Berko and J. Erskine (to be published) for Al taken at 77°K with 0.15-mrad slit widths. The computed curve misrepresents the contribution from the valence electrons in the core region because of the use of pseudopotential wave functions. (b) Angular distribution corresponding to free positrons annihilating in a gas of free electrons ($r_s=2$) of approximately the density as Al ($r_s=2.07$). The solid curve includes no correlation effects; the dashed curve includes the corrections described in Ref. 4.

$\sum_{\mathbf{K}} |a_{\mathbf{K}}|^2 = 1$. The high symmetry at $\mathbf{k}=0$ reduces the number of independent coefficients $a_{\mathbf{K}}$, thus facilitating the solution of Eq. (9) by allowing the inclusion of many plane waves without unduly increasing the size of the secular determinant. In the present work, for example, 145 plane waves were included in an 11×11 secular equation for Al. A 19×19 secular equation permitted consideration of 269 plane waves in Si.

Figure 3 shows the positron wave function of Al as a function of distance from the nucleus along the three principal cubic directions. The wave function is seen to exhibit substantial anisotropy in the region outside the ionic core. By contrast, in calculations employing the Wigner-Seitz method, such as those of Berko and Plaskett,[8] whose results are also shown in the figure, the positron wave function is required to be spherical throughout the cell by the boundary conditions. In addition, the amplitude closely approaches zero at the nucleus, as is expected on physical grounds. Since the high Fourier components $\mathbf{K}$ will contribute appreciably in this spatial region, this aspect of the numerical results illustrates that enough plane waves have been included to obtain good convergence.

In order to evaluate $f(\mathbf{p})$ as given by Eq. (1), one also requires explicit expressions for the electron wave functions $\psi_{\mathbf{k}l}$. For the valence electrons which contribute most significantly to the positron decay, these will be assumed to result from the solution of a pseudo-Hamiltonian which is characterized by a weak potential.[14] The expansion

$$\psi_{\mathbf{k}l}(\mathbf{r}) = \Omega^{-1/2}\sum_{\mathbf{K}} b_{\mathbf{K},l}(\mathbf{k})\, \exp[i(\mathbf{k}+\mathbf{K})\cdot\mathbf{r}], \quad (10)$$

therefore, includes relatively few plane waves. The omitted orthogonalization terms that involve the core wave functions are expected to play a small role, since the positron is effectively excluded from the core region by the Coulomb repulsion. This point will be discussed later in more detail.

Upon substituting (8) and (10), the valence contribution to Eq. (1) becomes

$$f^v(\mathbf{p}) = n_{\mathbf{p}/\hbar-\mathbf{G}} \left| \sum_{\mathbf{K},l} b_{\mathbf{K},l}(\mathbf{p}/\hbar-\mathbf{G})\, a_{\mathbf{G}-\mathbf{K}} \right|^2, \quad (11)$$

where G is the reciprocal lattice vector that translates $\mathbf{p}/\hbar$ into the first Brillouin zone. In nearly free-electron metals like Al, containing several valence bands, it is frequently more convenient to reexpress Eq. (11) in terms of the extended zone scheme:

$$f^v(\mathbf{p}) = \sum_{\mathbf{G}} n_{\mathbf{p}/\hbar-\mathbf{G}} \left| \sum_{\mathbf{K}} b_{\mathbf{K}}(\mathbf{p}/\hbar-\mathbf{G}) a_{\mathbf{G}-\mathbf{K}} \right|^2. \quad (12)$$

The summation over l is now replaced by one running over those $\mathbf{G}$ for which $\mathbf{p}/\hbar-\mathbf{G}$ lies within the Fermi surface.

To estimate the contribution of the core electrons, it is better to express $\psi_{\mathbf{k}l}(\mathbf{r})$ in terms of normalized atomic functions $\phi_c(\mathbf{r}-\mathbf{R})$, labeled by quantum numbers $c=(n, l, m)$ and centered on the lattice sites $\mathbf{R}$. The electron Bloch function is written in the tight-binding form

$$\psi_{\mathbf{k}c}(\mathbf{r}) = N^{-1/2}\sum_{\mathbf{R}} \exp(i\mathbf{k}\cdot\mathbf{R})\phi_c(\mathbf{r}-\mathbf{R}), \quad (13)$$

where N is the number of unit cells in the crystal. After decomposing the core function into a radial and spherical part $\phi_c(\mathbf{r}) = R_{nl}(r)\, Y_{lm}(\hat{r})$ and performing the angular integrations, the contribution of the core electrons for crystals containing one atom per unit

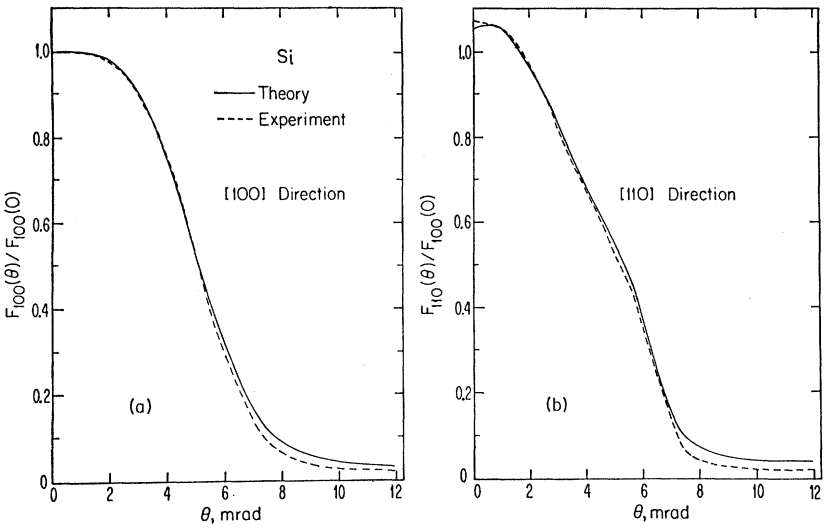

FIG. 5. Normalized computed and measured angular distribution of annihilation γ-ray pairs in Si along the [100] and [110] directions. The computed curves are based on the pseudopotential theory described in the text, and the experimental curves are those of Ref. 16. The error bars refer to the experimental data.

cell becomes

$$f^c(\mathbf{p}) = f_{nlm}(\mathbf{p}) = \frac{16\pi^2}{v_a} \left| \sum_{\mathrm{K}} a_{\mathrm{K}} I_{nl}(|\,\mathbf{p}/\hbar - \mathbf{K}\,|)\, Y_{lm}\,(\mathbf{p}/\hbar - \mathbf{K}) \right|^2, \tag{14}$$

where

$$I_{nl}(\mathbf{k}) = \int_0^\infty dr\, r^2 j_l(kr) R_{nl}(r)$$

and j_l is a spherical Bessel function.

It should be emphasized that the valence electrons' contribution in the core region is misrepresented in the present treatment because of the use of pseudo-wave-functions and the consequent omission of the terms that properly orthogonalize the valence and core wave functions. Within this approximation the total $f(\mathbf{p})$ as introduced in Eq. (1) is given by the sum of the valence and core contributions

$$f(\mathbf{p}) = f^v(\mathbf{p}) + f^c(\mathbf{p}). \tag{15}$$

It is similarly convenient to decompose the counting rate in the same way, by rewriting Eq. (2) in the form

$$F_{\mathrm{K}}(\theta) = F_{\mathrm{K}}{}^v(\theta) + F_{\mathrm{K}}{}^c(\theta). \tag{16}$$

III. ALUMINUM

The angular distribution of photon pairs produced by the annihilation of free zero-energy positrons in a free-electron gas has an inverse parabolic dependence[2,8,17]

$$F(\theta) \propto 1 - (\theta/\theta_F)^2.$$

Here $\theta_F = \hbar k_F/mc$. In a nearly free-electron metal like Al, this inverse parabola is superimposed on a smaller but considerably broader distribution arising from the core electrons and higher-momentum components of the valence electron and positron wave functions. As already indicated, these contributions are calculated only approximately or entirely neglected in the present treatment. This distribution was observed in Al by Berko and Plaskett.[8] In the same paper they presented an independent-particle theory in which the positron wave function was obtained in the Wigner-Seitz approximation using a potential arising from an Al^{+3} ionic core and three free valence electrons, and consistently with this, a free-particle wave function for the annihilated electron. The core electrons were treated in the tight-binding approximation. The agreement between the experimentally observed and theoretically calculated angular distributions was remarkably good.

The present calculations were undertaken primarily in order to study the effects the more refined methods for computing positron and electron wave functions described in the preceding section might have on the theoretical angular distributions arising from the parabolic region. The ground-state positron wave function was computed using x-ray form factors as measured by Batterman *et al.*[20] The conduction-band wave functions were taken to be the eigenfunctions of a pseudopotential Hamiltonian, and obtained by a method closely patterned after that originally proposed by Harrison.[14,21] According to this procedure, all V_{K}, with the exception of V_{111} and V_{200}, are neglected, and only the four lowest plane waves are included in the pseudo-wave-function. The two nonvanishing coefficients and the effective mass m^* were chosen to reproduce the bands obtained by Segall using the Korringa–Kohn–Rostoker method[22]: $V_{111} = 0.023$ Ry, $V_{200} = -0.043$ Ry, $m^*/m = 1.03$. Tight-binding functions were used for the core states. The radial functions were assumed to be adequately represented for the present purposes by the

[20] B. W. Batterman, D. R. Chipman, and J. J. DeMarco, Phys. Rev. **122**, 68 (1961).
[21] W. A. Harrison, Phys. Rev. **116**, 555 (1959).
[22] B. Segall, Phys. Rev. **124**, 1797 (1961).

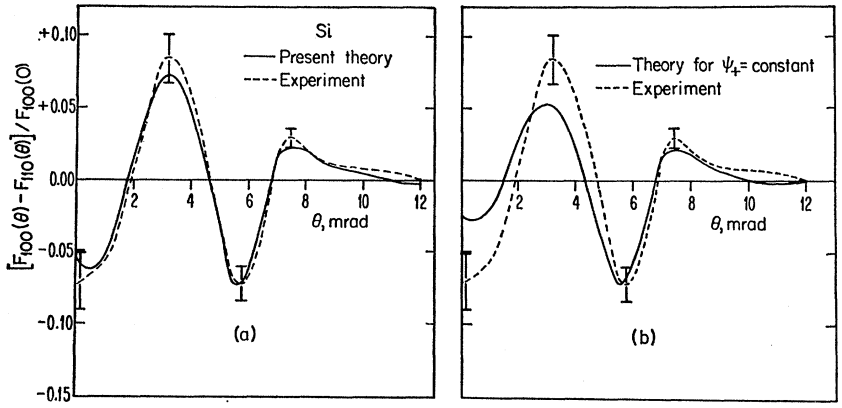

FIG. 6. Calculated anisotropy $(F_{100}(\theta)-F_{110}(\theta))/F_{100}(0)$ of the angular distribution in Si (solid curve) compared with experiment (dashed curve). (a) Pseudopotential theory using positron wave function computed as in Sec. II. (b) Same, using constant positron wave function. The contribution from the core electrons has been neglected in calculating this latter curve (cf. Ref. 27).

results of Herman and Skillman.[23,24] The integrated angular distribution [Eq. (2)] was computed for several crystal orientations, using a variable mesh that was densest in the region where the integrand $f(\mathbf{p})$ was most rapidly varying. The integrand was computed for an average of 200 points (p_x, p_y) per integral. The resultant $F(\theta)$ is precise to within 0.5%. The uncertainty, which prevails at all angles, arises from the rapid variation of $f(\mathbf{p})$ at the Fermi surface and the resultant difficulty in computing the contributions to the integrals coming from this region.

The results of this calculation, displayed in Fig. 4(a) for a [100] direction, show very close agreement with experiment which is not significantly different from the theoretical results of Berko and Plaskett.[8] Since the present method of calculation, in contrast to that of Ref. 8, also yields the anisotropy of $F_{\mathrm{K}}(\theta)$, the angular distribution was calculated for several different crystal orientations. The effect was found to be very small indeed, the difference between the curves corresponding to various orientations being within the experimental uncertainty of 1% of the maximum $F_{\mathrm{K}}(\theta)$.

Figure 4(b) shows the angular correlation for positron annihilation in a free-electron gas of approximately the same density as Al. The quantitative similarity of the angular correlation involving the valence electrons, which is nearly isotropic and quite apparently influenced very little by either the exclusion of the positron from the core or by the anisotropies of the positron and electron wave functions, is remarkable and deserves comment. Referring to the expression for $f^v(\mathbf{p})$ given in Eq. (12), we note that were the electrons truly free, $b_{\mathrm{K}}(\mathbf{k})=\delta_{\mathrm{K},0}$. Because of the nearly free-electron character of the valence electrons in Al, it is expected that $b_0(\mathbf{k})$ will be much larger than the other b_{K}'s over most of occupied $\mathbf{k}$ space. Despite the core exclusion and the anisotropy experienced by the positron wave function (cf. Fig. 3), a_0 in Al is also much larger than the remaining a_{K}: indeed $\sum_{\mathrm{K}\neq 0}|a_{\mathrm{K}}|^2<0.1$. The dominant contributions to $f^v(\mathbf{p})$ for $\mathbf{p}$ within the Fermi surface are exhibited by rewriting Eq. (12) as

$$f^v(\mathbf{p})=n_{\mathrm{p}/\hbar}\,|\,b_0(\mathbf{p}/\hbar)a_0\,|^2+\sum_{\mathrm{G}\neq 0}n_{\mathrm{p}/\hbar-\mathrm{G}}\,|\,b_0(\mathbf{p}/\hbar-\mathbf{G})a_{\mathrm{G}}\,|^2$$
$$+\sum_{\mathrm{K}\neq 0}n_{\mathrm{p}/\hbar-\mathrm{K}}\,|\,b_{\mathrm{K}}(\mathbf{p}/\hbar-\mathbf{K})a_0\,|^2$$
$$+\sum_{\mathrm{G}}n_{\mathrm{p}/\hbar-\mathrm{G}}\,|\sum_{\mathrm{K}\neq 0,\mathrm{G}}b_{\mathrm{K}}(\mathbf{p}/\hbar-\mathbf{G})a_{\mathrm{G}-\mathrm{K}}\,|^2. \quad (17)$$

For sufficiently small momenta $\mathbf{p}$, the first term on the right-hand side is dominant by far. The nonconstancy and anisotropy of the positron wave function, which are reflected principally in the second term, and the deviation of the electron wave function from its free-electron form whose influence is described by the third term, should have little effect if $\mathbf{p}$ is within the Fermi surface. Accordingly, the free-electron and positron description should be reasonable for the range of $\mathbf{p}$ in question.

By contrast, for $\mathbf{p}$ outside the Fermi surface, the first and previously dominant term in Eq. (17) drops out, since $n_{\mathrm{p}/\hbar}=0$, and the remaining terms, which contain the deviation from free-particle behavior, make the entire contribution. It is to be emphasized that the contribution of the core electrons must still be considered separately. However, it is seen from Fig. 4(a), which illustrates the results of the pseudopotential theory, that the terms of Eq. (17) under discussion account for nearly half the calculated magnitude of the tail. This theory, of course, includes only three plane waves of nonzero $\mathbf{K}$ in the wave functions of the valence electrons, and therefore does not treat accurately the third term on the right-hand side of Eq. (17). But the neglected high-$\mathbf{K}$ components correspond to rapid oscillations of the valence wave functions in the core region, and rough estimates suggest that the magnitude of their effect is less than 10% of the core contribution.

[23] F. Herman and S. Skillman, *Atomic Structure Calculations* (Prentice-Hall, Inc., Englewood Cliffs, N.J., 1963).

[24] The lack of self-consistency in the treatment of the core electrons is relatively unimportant since their contribution to the annihilation rate is small, and in any case cannot be separated from the contribution of the neglected higher-$\mathbf{K}$ components of the valence electrons.

TABLE I. Parameters for the three pseudopotentials discussed in the text. The last three columns indicate various valence-band separations corresponding to the three models. All entries are in Ry.

Pseudopotential	V_{111}	V_{220}	V_{311}	$\Gamma_{25'}-\Gamma_1$	$\Gamma_{25'}-X_4$	$\Gamma_{25'}-L_{3'}$
(1)	−0.21	+0.04	+0.08	+0.951	+0.242	+0.108
(2)	−0.21	+0.10	+0.05	+0.953	+0.281	+0.126
(3)	−0.21	+0.04	+0.05	+0.998	+0.265	+0.115

In solids like Si, where the pseudopotential coefficients are considerably larger, the first term in Eq. (17) no longer dominates to nearly the same extent as in Al. The discussion in Sec. IV will show the nonconstancy and anisotropy of the positron and electron wave functions to have considerable influence on the angular distribution in Si.

Figure 4(b) illustrates that the effect of electron-positron correlations on the γ-ray momentum distribution in Al is no greater than that of the periodic potential. This state of affairs is perhaps surprising, in view of the fact that correlations are known to have a large effect on the lifetime of positrons in Al,[8] but it is well in accord with existing many-body calculations. The work of Kahana,[4] which includes the effects of positron-electron correlations in free-electron metals by means of a dynamically screened Coulomb interaction, makes it possible to compute a momentum-dependent enhancement factor $\epsilon(p)=f_{\mathrm{MB}}(p)/f_{\mathrm{FE}}(p)$ at several electron densities. Here $f_{\mathrm{MB}}(p)$ is the many-body momentum distribution (though it includes no band effects) and $f_{\mathrm{FE}}(p)$ is the corresponding free-electron function, which is constant for all $p<p_F$. Since the resultant $\epsilon(p)$ can be fit very well by a simple polynomial of the form $\epsilon(p)=a+b\gamma^2+c\gamma^4$, with $\gamma=p/p_F$, it is possible to perform the necessary integrals and to obtain $F(\theta)$ including correlation corrections. The resulting curve is shown in Fig. 4(b) for $r_s=2$, very close to the actual Al r_s of 2.07. As is evident, the only effect of correlations on the curve is to create a very slight bulge in the free-electron parabola. At lower electron densities, Kahana's $\epsilon(p)$ results in a larger bulge. This is in accord with the experimental fact that positron-annihilation rates in free-electron metals deviate from the uncorrelated rates by a factor which increases with decreasing electron density.[2–7] More recent many-body calculations,[5,7] which include the effects of diagrams neglected by Kahana, do not alter this conclusion.

IV. SILICON

As already noted, solid-state effects enter much more significantly when positrons annihilate in a semiconductor like Si than in a free-electron metal like Al because the pseudopotential coefficients in the former are larger. The experimental angular distribution curves in semiconductors exhibit marked departures from the simple inverted parabola that characterizes the free-electron gas, and whose existence in metals permits the deduction of information concerning the Fermi surface. One might therefore expect that a theory involving electron and positron wave functions that properly reflect the potential and its crystalline anisotropies would be in better agreement with experiment than one that deals with the electrons appropriately, but treats the positrons in an approximation like that of Wigner and Seitz which neglects these anisotropies.

The calculations described in this section were carried out in fundamentally the same way as those of Al. X-ray form factors were obtained from the data of DeMarco and Weiss.[25] The method for calculating the positron wave function given in Sec. II required some modification since Si has the diamond structure and therefore contains two atoms per unit cell. Accordingly, Eq. (5) for the Fourier components of the positron potential became

$$V_{\mathrm{K}}=16\pi\rho_{\mathrm{K}}'\cos\tfrac{1}{2}\mathbf{K}\cdot\mathbf{b}/\mathbf{K}^2.$$

Here $\mathbf{b}$ is the vector connecting the two sublattices of the diamond structure and ρ_{K}' is the Fourier component of the charge density associated with one of the two sublattices. The group-theoretical reduction of the secular determinant (9) was also somewhat more complicated. The convergence of the plane-wave expansion for the positron wave function, Eq. (8), was slower than in Al: It was necessary to include 269 terms as compared to 145 in Al.

The wave functions for the valence electrons in Si were obtained as eigenfunctions of the pseudopotential band structure of Brust.[11] Only the lowest three pseudopotential coefficients are assumed to be nonvanishing. In Brust's scheme they take the values $V_{111}=-0.21$, $V_{220}=+0.04$, $V_{311}=+0.08$ Ry. Since these are relatively large, more plane waves than in Al are required to describe the pseudo-wave-functions adequately. Depending on $\mathbf{k}$, 15 to 25 are included directly, and a much larger number is considered by perturbation theory.

The more recent calculations of Kane obtain $\mathbf{k}$-dependent pseudopotential coefficients by the Heine-Abarenkov method[26] and retain six as nonvanishing. Since the valence bands, the only ones of importance here, are substantially the same as Brust's, one would expect Kane's theory to lead to annihilation curves very

[25] J. J. DeMarco and R. J. Weiss, Phys. Rev. **137**, 1869 (1965).
[26] V. Heine and I. Abarenkov, Phil. Mag. **9**, 451 (1964).

TABLE II. Angular distribution in Si for two different crystal orientations (subscripts) and the three pseudopotentials of Table I (superscripts). For each pseudopotential, the numbers are normalized so that $F_{100}(0)=1.000$. The positron wave function is calculated by the method of Sec. II. No core contribution is included. As is evident, the arbitrary changes in the electronic band structure given in Table I have no appreciable effect on the calculated angular distribution.

θ (mrad)	$F_{100}^{(1)}(\theta)$	$F_{100}^{(2)}(\theta)$	$F_{100}^{(3)}(\theta)$	$F_{110}^{(1)}(\theta)$	$F_{110}^{(2)}(\theta)$	$F_{110}^{(3)}(\theta)$
0.0	1.000	1.000	1.000	1.055	1.062	1.054
1.0	0.995	0.994	0.996	1.047	1.048	1.054
2.0	0.978	0.975	0.982	0.960	0.957	0.964
3.0	0.895	0.893	0.900	0.829	0.827	0.830
4.0	0.730	0.732	0.735	0.683	0.684	0.683
5.0	0.518	0.520	0.519	0.546	0.547	0.547
6.0	0.319	0.322	0.317	0.370	0.367	0.369
7.0	0.171	0.167	0.162	0.153	0.145	0.141
8.0	0.090	0.083	0.082	0.072	0.067	0.065
9.0	0.058	0.054	0.051	0.050	0.048	0.047
10.0	0.043	0.041	0.042	0.040	0.039	0.039
11.0	0.034	0.032	0.033	0.034	0.032	0.033
12.0	0.025	0.024	0.025	0.028	0.026	0.027

similar to those calculated here. Indeed, subsequent discussions will show the results to be quite insensitive to substantial variations in the pseudopotential coefficients.

The core contribution was computed, as in Al, by means of tight-binding functions for the core electrons. For the diamond structure, the equation analogous to (14) is

$$f_{nlm}(\mathbf{p})=\frac{32\pi^2}{v_a}\{|\sum_{\mathrm{K}}a_{\mathrm{K}}\cos\tfrac{1}{2}\mathbf{K}\cdot\mathbf{b}I_{nl}(|\mathbf{p}/\hbar-\mathbf{K}|)Y_{lm}(\mathbf{p}/\hbar-\mathbf{K})|_{\mathrm{B}}^2 + |\sum_{\mathrm{K}}a_{\mathrm{K}}\sin\tfrac{1}{2}\mathbf{K}\cdot\mathbf{b}I_{nl}(|\mathbf{p}/\hbar-\mathbf{K}|)Y_{lm}(\mathbf{p}/\hbar-\mathbf{K})|^2\}. \quad (18)$$

Here v_a is once again the volume of the unit cell. The core functions were taken from the tables of Herman and Skillman.[23]

Figures 5(a) and 5(b) show the computed and the measured $F_{\mathrm{K}}(\theta)$ along the [100] and [110] directions. The two experimental curves have been normalized to equal area, i.e., to equal total annihilation rate, and the theoretical and experimental $F_{100}(0)$ have been set equal. The function $f^v(\mathbf{p})$ was computed on a cubic mesh of density $1/(\pi/4a)^3$, where a represents the fcc cube edge, and $f^c(\mathbf{p})$ was assumed spherically symmetric and computed along the [100] direction. Because of the absence of partially filled bands, $f(\mathbf{p})$ experiences no discontinuity. As a result, it is more slowly varying and the resulting integrals are precise to four figures, a considerable improvement over Al. The core contribution $F^c(\theta)$ is found to be quite small and never amounts to more than 6% of the maximum value of $F(\theta)$.

The excellent agreement between theory and experiment is perhaps more dramatically illustrated in Fig. 6(a), where the "anisotropy" $(F_{100}(\theta)-F_{110}(\theta))/F_{100}(0)$ has been plotted for both.

Because of the remarkable agreement of the one-particle theory with experiment, several additional calculations were undertaken in order to ascertain the degree to which the present results are sensitive to the positron and electron wave functions. In Fig. 6(b) the "anisotropy" is shown for the situation corresponding to constant positron wave function and the same valence-electron wave functions as in Fig. 6(a). The core contribution was neglected in this calculation.[27] It is evident that the agreement between theory and experiment is not as good as in Fig. 6(a). The qualitative features of the curve are, however, reproduced, indicating that they arise primarily from the anisotropy of the electron wave functions.

A corresponding test of the sensitivity of the results to the electronic wave functions was made by deliberately distorting the valence bands by means of arbitrary and unphysical changes in the pseudopotential coefficients. Two additional sets of pseudopotential coefficients are listed in Table I, together with the

[27] If the core contribution had been computed with a constant positron wave function, its effect would have been greatly exaggerated because the amplitude of this wave function in the core is far too large. The apparent inconsistency in comparing a curve that includes a core contribution with one that does not is not relevant to the present comparison. If the exaggerated core contribution had been included in the calculation involving the constant positron wave function, its effect would have been to reduce the anisotropy because the core contribution is isotropic. The discrepancy with experiment would thus have been rendered even greater.

Brust coefficients. Some typical valence-band energies at points of high symmetry in the Brillouin zone referred to the band maximum at Γ are given in the last three columns of the table. The first of these is characteristic of the total valence-band width and the last two describe the energy variation of the uppermost band along [100] and [111] directions, respectively. As is apparent, the changes induced by the new pseudopotentials are small compared to the total valence-band width of about one rydberg. The pseudopotential denoted in the table as (2) has the effect of broadening the upper valence band relative to the Brust pseudopotential (1) without changing the total width. The pseudopotential (3) increases the width but affects the curvature of the upper valence band less than (2).

It is worth noting that these changes in the pseudopotential coefficients affect the conduction bands much more markedly than they do the valence bands. This relative insensitivity of the valence-band energies to the pseudopotential coefficients, which was previously noted by Cohen and Bergstresser,[12] is consistent with the insensitivity of the corresponding angular-distribution curves, which reflect only the valence-band structure.

Table II exhibits numerically the angular distribution corresponding to an x-ray positron wave function and the electron pseudo-wave-functions associated with the three pseudopotentials of Table I. No core contribution has been included, and for all three pseudopotentials the value of $F_{100}(0)$ has been set equal to 1.000. It is apparent that the annihilation curves corresponding to the three pseudopotentials are practically identical, thus confirming that the stability of the valence-band structure to changes in the pseudopotential coefficients is reflected in a similar stability of the annihilation curves.

The insensitivity of the annihilation curves to these quite arbitrary changes in the pseudopotential is at first sight disappointing, since it indicates that positron-annihilation experiments are not a fruitful source of detailed information about the band structure of semiconductors. But the very precision with which the band effects can be taken into account makes Si an excellent subject for the study of the effects of electron-positron correlations on the annihilation rate. Such a study would be of particular interest in view of the fact that nearly all such theoretical investigations have so far concentrated on metals.

Since the experimental angular-distribution curves in Si exhibit considerably more structure than those of Al, the fact that they agree well with curves calculated using pseudopotential wave functions for the valence electrons provides much stronger evidence than do the Al calculations that this approach is useful for a variety of solids. The applicability of pseudopotential wave functions is already evident in the work of Erskine and McGervey,[15] in which experimental results for Si were interpreted with some success in terms of a nearly free-electron approximation with a single nonvanishing pseudopotential coefficient.

The fact that angular-correlation curves in Si are derivable from an independent-particle theory implies that the principal task remaining for a many-body theory is to explain the observed annihilation rate. Here it is relevant to compare Si with Al. Al has a slightly lower electron density ($r_s=2.07$) than Si ($r_s=2.01$). Nonetheless, in contrast to the predictions of theories considering positrons in an electron gas, the annihilation rate is higher in Al than in Si by about 10%.[28] This effect possibly results from the presence of the band gap in Si. If the positron is considered an external perturbation, then since there are states available at the Fermi surface, the electrons in Al can easily respond to it by increasing the local density of particles with which the positron can annihilate. The corresponding screening effect would be expected to be smaller in a semiconductor like Si because there are no available states near the Fermi surface.

ACKNOWLEDGMENTS

We are grateful to S. Berko for stimulating our interest in this subject, for a number of fruitful discussions, and for making the data quoted in Fig. 4 available prior to publication. B. Segall kindly made available some of the wave functions obtained in his Al calculations, which were most helpful in early stages of this work. Conversations with A. R. Williams are also much appreciated.

[28] H. Weisberg and S. Berko, Phys. Rev. **154**, 249 (1967).